

Different methods to fabricate efficient planar perovskite solar cells based on solution-processing Nb₂O₅ as electron transporting layer

Heng Guo¹, Jian Yang¹, Bingxue Pu¹, Haiyan Zhang¹, and Xiaobin Niu^{1,2,*}

¹State Key Laboratory of Electronic Thin Film and Integrated Devices, University of Electronic Science and Technology of China, Chengdu, China

²Institute of Fundamental & Frontier Science, University of Electronic Science and Technology of China, Chengdu, China

*Corresponding author e-mail: xbnui@uestc.edu.cn

Abstract. Organo-lead perovskites as light harvesters have represented a hot field of research on high-efficiency perovskite solar cells. Previous approaches to increasing the solar cell efficiency have focused on optimization of the morphology of perovskite film. In fact, the electron transporting layer (ETL) also has a significant impact on solar cell performance. Herein, we introduce a facile and low temperature solution-processing method to deposit Nb₂O₅ film as ETL for PSCs. Based on Nb₂O₅ ETL, we investigate the effect of the annealing time for the perovskite films via different solution processing, relating it to the perovskite film morphology and its influence on the device working mechanisms. These results shed light on the origin of photovoltaic performance voltage in perovskite solar cells, and provide a path to further increase their efficiency.

1. Introduction

Organic-inorganic hybrid perovskites (typically, MAPbI₃, MA = CH₃NH₃⁺) were first incorporated into photovoltaic devices with the power conversion efficiency (PCE) of 3.8% [1]. In just a few years, the perovskite solar cells (PSCs) has achieved high PCE rapidly approaching 22.1% [2] via solvent engineering, due to the outstanding optoelectronic properties of the perovskite materials [3]. However, for PSC devices to work to their full potential, recent efforts in this field have therefore focused on the synthesis and development of suitable hole transport layers (HTLs) and electron transport layers (ETLs). So far, the record top-performing PSCs employ compact or mesostructured titanium dioxide (TiO₂) as ETL in the mesoscopic type devices [4], although the use of other oxide materials, such as ZnO, SnO₂, Nb₂O₅ and Zn₂SnO₄ and BnSnO₄, has been reported [5]. Interestingly, niobium oxide (Nb₂O₅) is an n-type semiconductor with improved UV-stability relative to that of TiO₂ [6]. However, Nb₂O₅ can only be deposited in PSCs using magnetron sputtering technique [7].

Herein, a facile and low temperature solution-processing method is applied to deposit Nb₂O₅ as ETL for PSCs. Based on Nb₂O₅ ETL, we investigate the effect and importance of the annealing time during the final conversion step, relating it to the perovskite film morphology and its influence on the device working mechanisms.



2. Experimental

2.1. Device Fabrication

The illustration of the one-step and two-step process to prepare perovskite solar cells is presented in Figure 1. The Nb₂O₅ nanocrystals were dispersed into anhydrous chloroform and methanol (EE). The obtained suspension spin-coated onto FTO substrates and annealed at 150°C for 60 min. One-step spin-coating method: The MAPbI₃ precursor solution was prepared by mixing 1 M PbI₂ and MAI at 1:1 molar ratio in DMF. The precursor solution was spin-coated at 4000 r.p.m. for 40 s. During this procedure, 80 µL of chlorobenzene was pipetted onto the spinning substrate after 12 s. The spin-coated substrates were then dried at 100 °C for 15, 35, 65, 95, and 125 min, respectively (One-step TA). Two-step spin-coating method: 45 µL of 1 M PbI₂/DMF solution was spin-coated on the Nb₂O₅ layer successively at 4000 r.p.m. for 40 s. After spin-coating, the films were annealed at 100 °C for 5 min. Then the samples were cooled to room temperature. The 45 µL of MAI solution (1 M in ethanol) was loaded on the PbI₂ layer for 5 s to react with PbI₂ and form MAPbI₃, and subsequently spun at 3500 r.p.m. for 40 s and annealed at 100 °C for 15, 35, 65, 95, and 125 min, respectively (Two-step TA). Besides, during above-mentioned procedure, 10 µL of DMF was added to the edge of the petri dish when the annealing started (Two-step SA). After cooling down to room temperature, the HTL was subsequently deposited on top of the perovskite film by spin coating at 4000 rpm for 30 s using a chlorobenzene solution which contained 72 mg/mL of Spiro-OMeTAD and 28 µL/mL of tert-butylpyridine, as well as 18 µL/mL of bis(trifluoromethane)sulfonimide lithium salt (520 mg/mL in acetonitrile). Finally, 100-nm Au electrodes were deposited through a shadow mask, defining a device area of 0.13 cm², by thermal evaporation.

2.2. Characterization

Scanning electron microscope (SEM, JSM, 6490LV) were investigated to the morphology of the perovskite samples. The as-prepared perovskite films were characterized by X-ray diffraction (XRD, Rigaku RINT2400, Japan) with Cu K α ($\lambda = 0.1541$ nm) radiation at 45 kV and 40 mA. The current density–voltage (J–V) curves were measured under simulated one-sun AM 1.5G illumination (100 mW·cm⁻²) using a solar simulator (SAN-EI, AAA grade, Newport Corporation) with a Keithley 2400 Source Meter under an N₂ atmosphere. The light intensity was calibrated with a Si reference cell.

3. Results and discussion

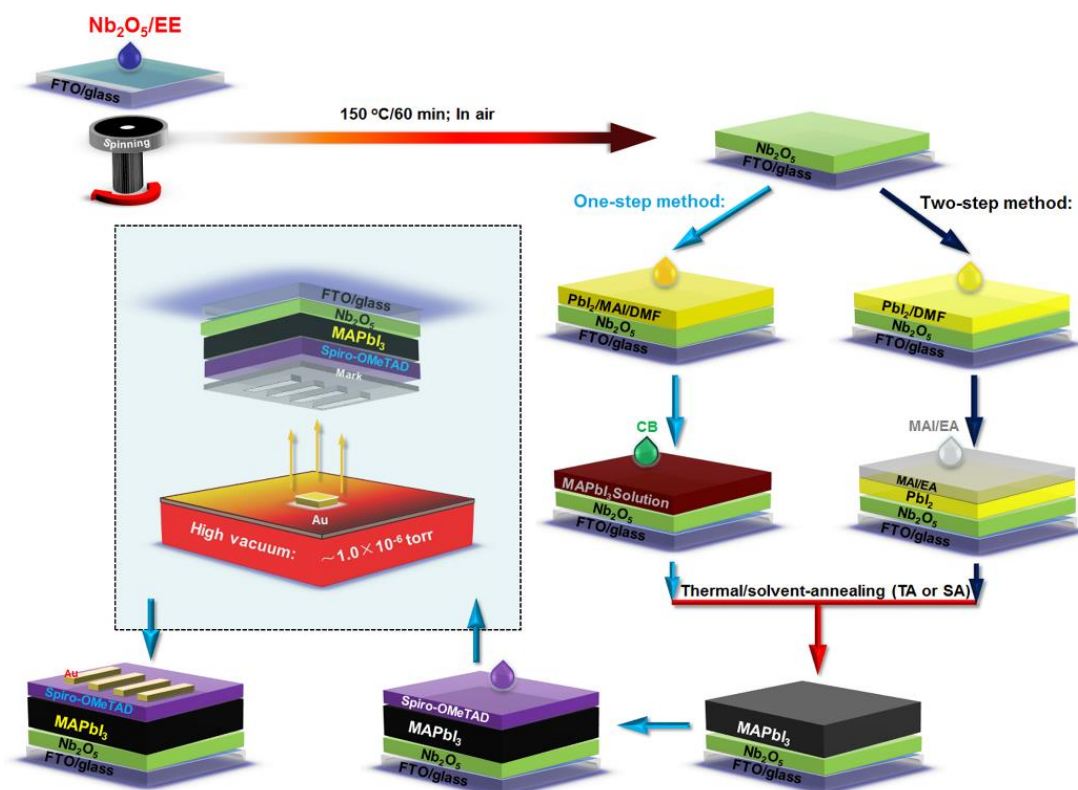


Figure 1. Illustration of the one-step and two-step process to prepare perovskite solar cells.

Figure 2 shows the SEM images of the perovskite films deposited on Nb₂O₅/FTO substrate by using different solution-processing methods. As illustrated in Figure 2a, the perovskite films exhibited an amorphous morphology with a variety of pores distributed over the surface. It is clearly seen that the numbers of the pore decrease with the increasing of the annealing time. In Figure 2b, the films exhibited the unique morphology with many crystalline grains and the grain size of the perovskite film was increased when the annealing time increased. The reasons is that large perovskite grains were grown by solvent annealing that facilitated grain boundary migration by the solvent vapors [8]. As shown in Figure 2c, the film showed uniform polygon grains of several hundred nanometers, which were comparatively smaller than that of perovskite film obtained by Two-step TA method (Figure 2d). It is notable that the MAPbI₃ do form continuous and dense films by One-step TA method. Therefore, we observed the same morphology of perovskite on the Nb₂O₅ substrates, which well agrees with the perovskite based on the TiO₂ layer [9,10]. Moreover, the morphology of the perovskite observed for the Nb₂O₅ interface do correlate well with the solution-processing method and annealing time.

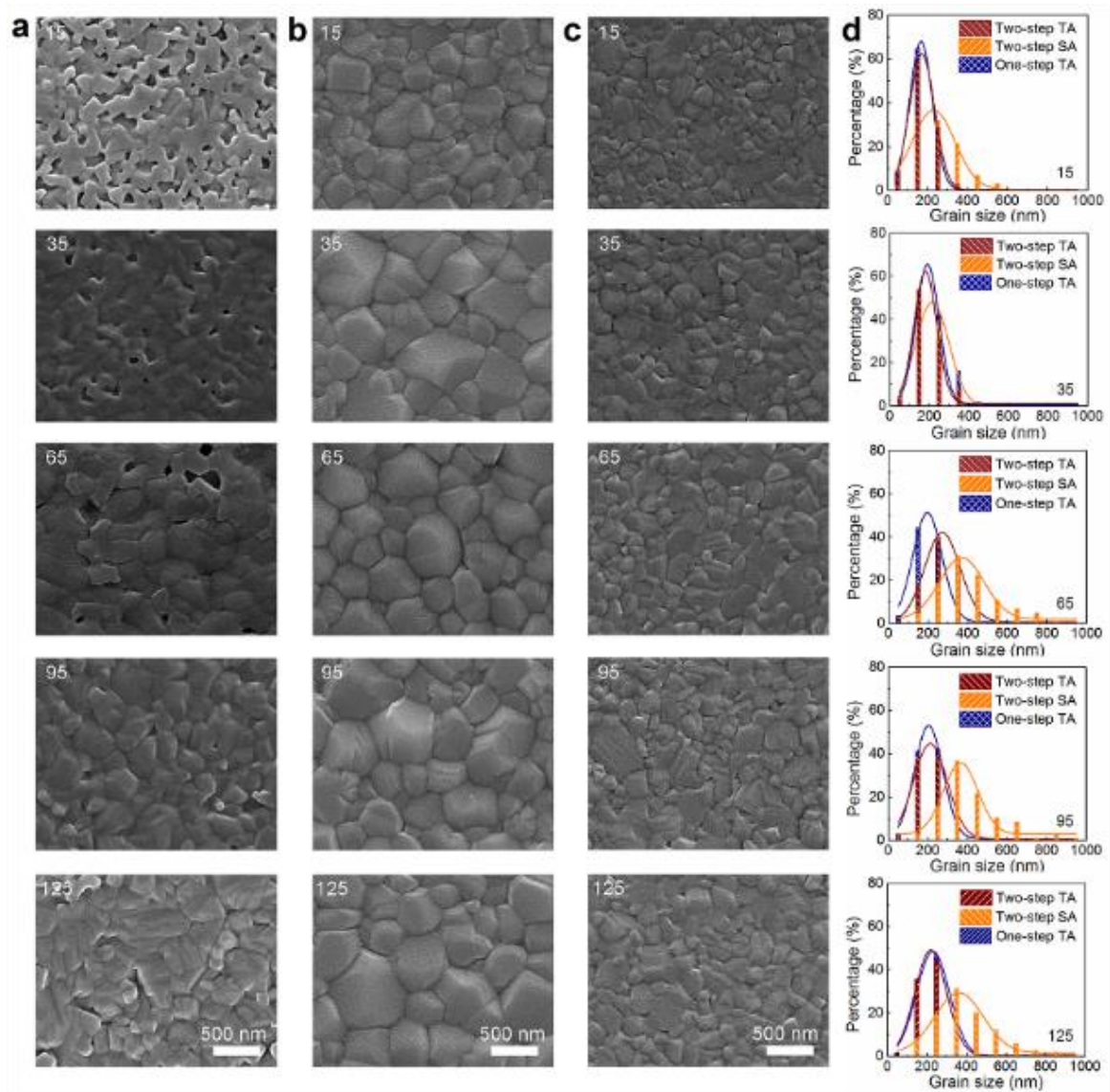


Figure 2. SEM images of perovskite films prepared by (a) Two-step TA, (b) Two-step SA and (c) One-step TA methods. (d) Grain size distributions of perovskite films prepared by three methods. The same scale bar and label applied to all images in a column and the numbers represent the annealing time.

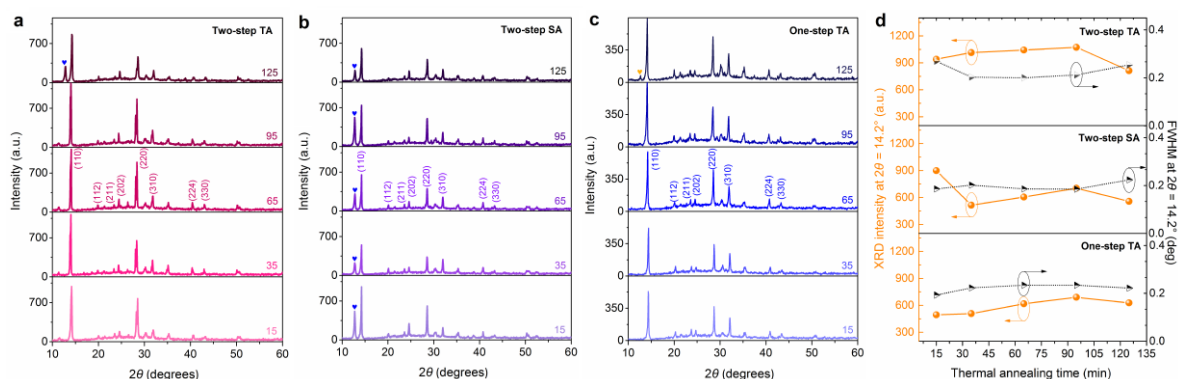


Figure 3. XRD patterns of perovskite films prepared by (a) Two-step TA, (b) Two-step SA and (c) One-step TA methods. (d) Variation of XRD peak intensity at $2\theta = 14.2^\circ$ (110) and corresponding FWHM evolution with the increasing annealing time.

In order to understand the formation and evolution of perovskite film by different solution-processing methods with the annealing time, XRD curves of the films has been carried out in Figure 3a-b. Normally, these perovskites films exhibit strong characteristic diffraction patterns for $\text{CH}_3\text{NH}_3\text{PbI}_3$ tetragonal crystal structure [11]. Thus, there is an additive peak observed at 12.2° for the perovskite prepared by using Two-step SA method, which can be matched well with the (001) lattice plane of crystallized PbI_2 . [12] This may be related to the strong effect of the solvent vapor in thermal annealing. It should be noted that the relative intensity of (110) diffraction peak ($2\theta = 14.2^\circ$) can be relative to different annealing time (Figure 3d).

By applying Nb_2O_5 as ETLs, a typical configuration of FTO/ Nb_2O_5 /Perovskite/Spiro-OMeTAD/Au used for the planar PSCs in this work. Figure 4 summarizes the photovoltaic parameters of PSCs based on the preparation of perovskite by using solution-processing methods. Upon increasing the annealing time in three solution-processing methods, the PCE first augments and subsequently decrease with a peak at the annealing time = 95 min. As shown in Figure 4a, the representative device based on Two-step TA with the 65 min annealing time presents an open-circuit voltage (V_{oc}) = 0.81 V, a short-circuit current density (J_{sc}) = 16.1 mA cm^{-2} , and a Fill Factor = 68 %, corresponding to a PCE of 8.9 %, a superior photovoltaic performance than that of the devices applying Two-step SA and one-step TA method. Obviously, the PCE improvement can be related to the suitable annealing time by using all the solution-processing methods.

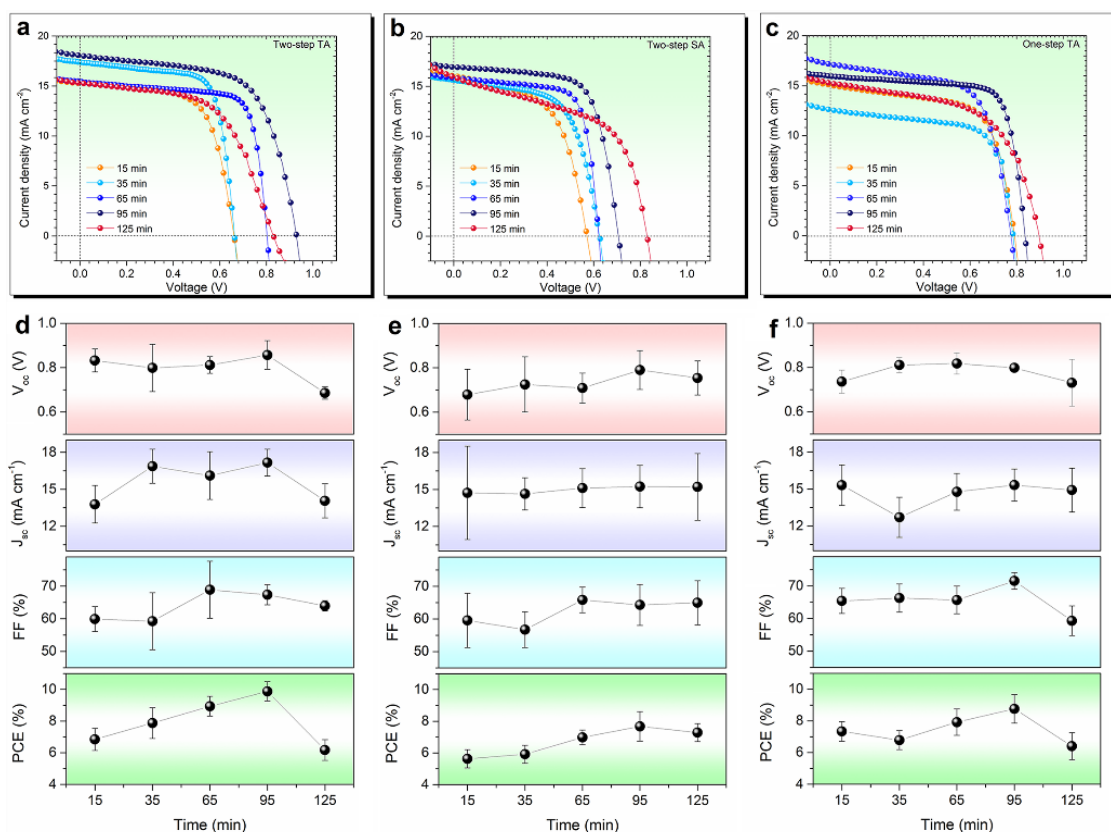


Figure 4. The current density-voltage (J - V) curves of PSCs based on the preparation methods of perovskite by using (a) Two-step TA, (b) Two-step SA and (c) One-step TA. Photovoltaic metric of devices plotted as function of the annealing time with three preparation methods: (d) Two-step TA, (e) Two-step SA and (f) One-step TA.

4. Conclusion

In summary, we identified an efficient method to prepare Nb₂O₅ as useful electro transporting layer. Based on Nb₂O₅ ETL, we studied the properties of the MAPbI₃ perovskite films under the influence of the annealing time, which can be generated under three solution processing methods. We found that the annealing time had an influence in the perovskite film morphology. Further study demonstrated that our Nb₂O₅-based solar cells are obtained with a stabilized PCE of > 8 %. The devices can be easily processed under low temperature, which will have important fundamental implications on the development of more efficient perovskite solar cells. These results shed light on the origin of photovoltaic performance in perovskite solar cells, and provide a path to further increase their efficiency.

Acknowledgments

This work was financially supported by the National Natural Science Foundation of China (Grant Nos. 11104010 and 61474014).

References

- [1] A. Kojima, K. Teshima, Y. Shirai, T. Miyasaka, Organometal halide perovskites as visible-light sensitizers for photovoltaic cells, *J. Am. Chem. Soc.* 131 (2009) 6050-6051.
- [2] W.S. Yang, B.W. Park, E.H. Jung, N.J. Jeon, Y.C. Kim, D.U. Lee, S.S. Shin, J. Seo, E.K. Kim, J.H. Noh, S.I. Seok, Iodide management in formamidinium-lead-halide-based perovskite

- layers for efficient solar cells, *Science* 356 (2017) 1376-1379.
- [3] J. You, L. Dou, K. Yoshimura, T. Kato, K. Ohya, T. Moriarty, K. Emery, C.C. Chen, J. Gao, G. Li, Y. Yang, A polymer tandem solar cell with 10.6% power conversion efficiency, *Nat. Commun.* 4 (2013) 1446.
- [4] H. Kim, K.G. Lim, T.W. Lee, Planar heterojunction organometal halide perovskite solar cells: roles of interfacial layers, *Energy Environ. Sci.* 9 (2016) 12-30.
- [5] S.S Shin, E.J. Yeom, W.S. Yang, S. Hur, M.G. Kim, J. Im, J.W. Seo, J.H. Noh, S. Seok, Colloidally prepared La-doped BaSnO₃ electrodes for efficient, photostable perovskite solar cells, *Science* 356 (2017) 167.
- [6] J. Barbe, M.L. Tietze, M. Neophytou, B. Murali, E. Alarousu, A.E. Labban, M. Abulikemu, W. Yue, O.F. Mohammed, I. McCulloch, A. Amassian, S. Del Gobbo, Amorphous tin oxide as a low-temperature-processed electron-transport layer for organic and hybrid perovskite solar cells, *ACS Appl. Mater. Interfaces*, 9 (2017) 11828-11836.
- [7] N. Usha, R. Sivakumar, C. Sanjeeviraja, M. Arivanandhan, Niobium pentoxide (Nb₂O₅) thin films: Power and substrate temperature induced changes in physical properties, *Optik* 126 (2015) 1945-1950.
- [8] C. Bi, B. Chen, H. Wei, S. DeLuca, J. Huang, Efficient flexible solar cell based on composition-tailored hybrid perovskite, *Adv. Mater.* 29 (2017) 1605900.
- [9] Y. Hou, W. Chen, D. Baran, T. Stubhan, N.A. Luechinger, B. Hartmeier, M. Richter, J. Min, S. Chen, C.O. Quiroz, N. Li, H. Zhang, T. Heumueller, G.J. Matt, A. Osvet, K. Forberich, Z.G. Zhang, Y. Li, B. Winter, P. Schweizer, E. Spiecker, C.J. Brabec, Overcoming the interface losses in planar heterojunction perovskite-based solar cells, *Adv. Mater.* 28 (2016) 5112-5120.
- [10] X. Ling, J. Yuan, D. Liu, Y. Wang, Y. Zhang, S. Chen, H. Wu, F. Jin, F. Wu, G. Shi, X. Tang, J. Zheng, S.F. Liu, Z. Liu, W. Ma, Room-temperature processed Nb₂O₅ as the electron-transporting layer for efficient planar perovskite solar cells, *ACS Appl. Mater. Interfaces* 9 (2017) 23181-23188.
- [11] Y. Liu, Z. Yang, D. Cui, X. Ren, J. Sun, X. Liu, J. Zhang, Q. Wei, H. Fan, F. Yu, X. Zhang, C. Zhao, S.F. Liu, Two-inch-sized perovskite CH₃NH₃PbX₃ (X = Cl, Br, I) crystals: Growth and characterization, *Adv. Mater.* 27 (2015) 5176-5183.
- [12] L. Zhao, D. Luo, J. Wu, Q. Hu, W. Zhang, K. Chen, T. Liu, Y. Liu, Y. Zhang, F. Liu, T.P. Russell, H.J. Snaith, R. Zhu, Q. Gong, High-performance inverted planar heterojunction perovskite solar cells based on lead acetate precursor with efficiency exceeding 18%, *Adv. Funct. Mater.* 26 (2016) 3508-3514.